



■ BONE FRACTURE

Unbiased gene expression analysis of the delayed fracture healing observed in Zucker diabetic fatty rats

**J. Sung,
K. R. Barratt,
S. M. Pederson,
C. Chenu,
I. Reichert,
G. J. Atkins,
P. H. Anderson,
P. J. Smitham**

From Adelaide Medical School, Adelaide, Australia

Aims

Impaired fracture repair in patients with type 2 diabetes mellitus (T2DM) is not fully understood. In this study, we aimed to characterize the local changes in gene expression (GE) associated with diabetic fracture. We used an unbiased approach to compare GE in the fracture callus of Zucker diabetic fatty (ZDF) rats relative to wild-type (WT) littermates at three weeks following femoral osteotomy.

Methods

Zucker rats, WT and homozygous for leptin receptor mutation (ZDF), were fed a moderately high-fat diet to induce T2DM only in the ZDF animals. At ten weeks of age, open femoral fractures were simulated using a unilateral osteotomy stabilized with an external fixator. At three weeks post-surgery, the fractured femur from each animal was retrieved for analysis. Callus formation and the extent of healing were assessed by radiograph and histology. Bone tissue was processed for total RNA extraction and messenger RNA (mRNA) sequencing (mRNA-Seq).

Results

Radiographs and histology demonstrated impaired fracture healing in ZDF rats with incomplete bony bridge formation and an influx of intramedullary inflammatory tissue. In comparison, near-complete bridging between cortices was observed in Sham WT animals. Of 13,160 genes, mRNA-Seq analysis identified 13 that were differentially expressed in ZDF rat callus, using a false discovery rate (FDR) threshold of 10%. Seven genes were upregulated with high confidence (FDR = 0.05) in ZDF fracture callus, most with known roles in inflammation.

Conclusion

These findings suggest that elevated or prolonged inflammation contributes to delayed fracture healing in T2DM. The identified genes may be used as biomarkers to monitor and treat delayed fracture healing in diabetic patients.

Cite this article: *Bone Joint Res* 2023;12(10):657–666.

Keywords: Fracture healing, Fracture nonunion, Zucker rats, Type 2 diabetes mellitus

Article focus

■ To investigate messenger RNA (mRNA) gene expression (GE) in the fracture callus of diabetic and control rats three weeks post-femoral osteotomy.

fatty (ZDF) compared to wild-type (WT) samples.

■ Delayed fracture healing in diabetic patients may be related to increased proinflammatory GE.

Key messages

■ Fracture healing was delayed in diabetic rats, indicated by histological and radiological analysis.
■ Unbiased mRNA sequencing identified potentially causative elevated proinflammatory GE patterns in Zucker diabetic

Strengths and limitations

■ Unbiased GE analysis identified differentially expressed genes in the fracture callus of ZDF rats compared to WT, providing new insight into the pathogenesis of delayed fracture healing in type 2 diabetes mellitus.

Correspondence should be sent to Peter J. Smitham; email: petersmitham@gmail.com

doi: 10.1302/2046-3758.1210.BJR-2023-0062.R1

Bone Joint Res 2023;12(10):657–666.

- This study could not determine if GE changes were the cause of the impaired fracture healing observed.

Introduction

Type 2 diabetes mellitus (T2DM) is a metabolic disease characterized by chronic hyperglycaemia, leading to decreased sensitivity to insulin. According to the World Health Organization (WHO), more than 422 million people currently have diabetes, with increasing prevalence and mortality.¹ Among its many complications, T2DM is known to pose a higher risk for fracture, particularly for hip fracture, and is associated with delayed fracture healing.² In diabetic patients, fracture healing can be prolonged by 87%,³ with increased risk of other orthopaedic complications such as delayed union, nonunion, dislocation, or pseudoarthrosis.^{4,5}

The detrimental effect of T2DM on the regenerative ability of bone is postulated to be acting at cellular, molecular, and biomechanical levels.⁶ This includes increased osteoclastogenesis and prolonged and elevated inflammation, with difficulty downregulating inflammation once induced.⁷⁻⁹ A variety of pharmacological treatments are available to control blood glucose levels, including metformin, sulfonylurea, and insulin.¹⁰ However, there is no specific treatment to normalize fracture healing in diabetic patients.

Previous studies have examined gene expression (GE) associated with T2DM in patient-derived tissues, such as peripheral blood and skeletal muscle.^{11,12} The Zucker diabetic fatty (ZDF) rat is a useful experimental model of human T2DM. ZDF rats carry recessive *fa/fa* mutation for the leptin membrane receptor, which results in a shortened leptin-receptor protein that does not interact with leptin effectively.¹³ Animals homozygous for the *fa* allele become noticeably obese by three to five weeks of age, becoming hyperlipidaemic, hypercholesterolaemic, hyperinsulinaemic, and developing adipocyte hypertrophy and hyperplasia.¹⁴ Liu et al¹⁵ observed an upregulation of ANXA3 in patients with T2DM and fracture nonunion, leading to the conclusion that elevated ANXA3 expression potentially contributes to fracture nonunion in T2DM by modulating neutrophil activity. Although research involving altered expression of microRNA during fracture healing in diabetic rats has been performed previously,¹⁶ to our knowledge specific messenger RNA (mRNA) expression during fracture healing in ZDF rats has not been reported.

This study aimed to improve the molecular understanding of the pathophysiology of delayed fracture healing in diabetes by examining the differential GE in the fracture callus of ZDF compared to wild-type (WT) littermate controls.

Methods

Animals. The authors of this study adhered to the ARRIVE guidelines for reporting in vivo experiments. We selected a small sample size because the mRNA GE in fracture callus of ZDF rats was evaluated in vivo for the first time.

Therefore, the purpose was to gather basic evidence regarding the specific GE seen in the diabetic cohort. A total of 20 rats, consisting of 14 male ZDF (ZDF-Lepr^{fa/fa}) and six leptin receptor-intact Zucker rats (ZDF-Lepr^{+/+}), were randomly assigned to the diabetic and control groups, respectively. From four weeks of age, all were fed a high-fat (7.55%) diet (SF06-019, Purina 5008 Equivalent; Speciality Feeds, Australia) ad libitum. At ten weeks of age, rats were subjected to a mid-diaphyseal transverse osteotomy in the left femur, as described below. Three weeks after osteotomy, animals were culled by CO₂ exposure and cervical dislocation and the femora were removed for analysis. At the experiment end, the mean weight of ZDF rats was 546.8 g (standard deviation (SD) 27.5), compared to control rats, which weighed an average of 349.5 g (SD 4.0), confirming the differential acquisition of a diabetic phenotype in the ZDF group. This study was approved by the University of South Australia Animal Ethics Committee (Approval No. U15-16).

Surgical procedure. All procedures were performed using a previously reported technique.¹⁷ Briefly, the left leg area where the surgery was performed was shaved, and the limb was cleaned using ethanol and betadine. A 3- to 4-cm curved incision was made through the skin parallel to the femur. An incision was then made through the fascia, and blunt dissection was used to separate the muscles to expose the femur. An external fixation device to the left femur was applied using a non-articulating fixator by hand-drilling four 1 mm holes in the cortical bone, so as not to cause overheating (and necrosis) of the surrounding tissue. Threaded stainless steel pins (1.2 mm diameter) were inserted into these holes. The original curved incision was made to stretch the skin and fit over the surgical site with the pins in situ. This also resulted in the incision being suitably distant from the pins to minimize the risk of infection. An external fixator device was then fitted to interlock the pins securely. Mid-diaphyseal transverse osteotomy in the left femur was performed using a diamond-tipped bone hand saw, and a 1 mm gap was created. Finally, the incised muscle and skin were sutured, and Betadine solution was applied to sterilize the wound. Vetergesic (0.1 cc; Alstoe, UK) for analgesia and cephalosporin (0.05 cc; Sandoz Ltd, UK) were given postoperatively for one day to prevent infection, and the animals were then returned to their cages. The external fixator remained attached, effectively keeping the fractured bone aligned and supported for the postoperative period. Due to the gross weight and size difference of the two groups of rats, the surgeon (PJS) could not be completely blinded to whether the animals operated on were from a diabetic or a control group.

Radiological analysis of fracture repair. Once the animals were culled, dual energy X-ray absorptiometry (DXA) radiographs of the osteotomized femur were acquired using a Faxitron cabinet (Hologic, USA). Radiological images were evaluated for evidence of fracture healing and fracture union, which was defined as bridging of the fracture by bone, callus, or trabeculae, bridging of the

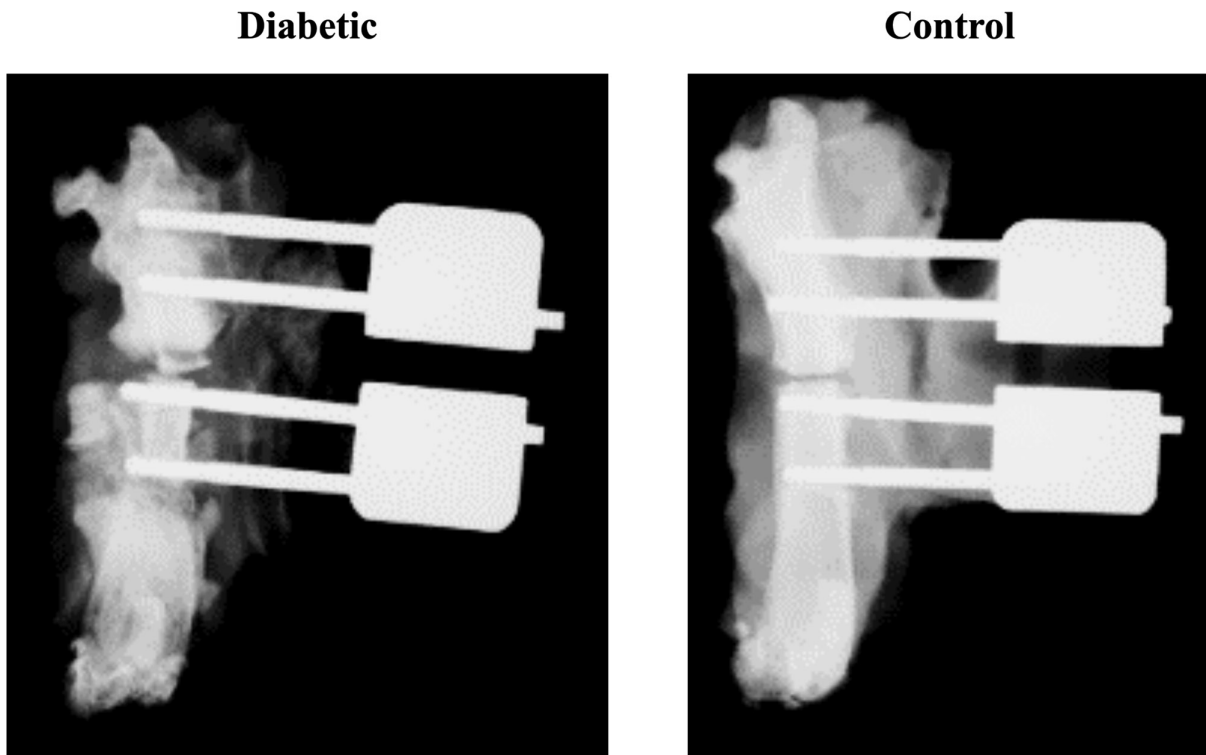


Fig. 1

A representative radiograph showing fracture healing of the type 2 diabetes mellitus group compared to non-diabetic controls three weeks post-femoral osteotomy, with external fixators in situ.

fracture at three of four cortices, and obliteration of the fracture line and/or cortical continuity.

Histology of fracture sites. For histology, non-decalcified sagittal sections of the femur were prepared from formalin-fixed, polymethyl methacrylate (PMMA) resin-embedded bone as previously described,¹⁸ and stained with Toluidine blue.¹⁹ Histological sections were imaged using a digital slide scanner (NanoZoomer 2.0-HT; Hamamatsu Photonics, Japan).

Gene expression analysis. For GE analysis, whole femora ($n = 3/\text{group}$) were submerged in ten volumes of RNeasy Lysis Buffer (Qiagen, Crawley, Australia), and stored overnight at 4°C before freezing at -80°C. Frozen whole femora were then pulverized before extraction of total RNA using the TRIzol extraction method, as previously described.²⁰

Following RNA purification, rat total mRNA sequencing (mRNA-Seq) was performed (Australian Genome Research Foundation, Australia). Sequencing data quality was assessed using ngsReports,²¹ with reads being trimmed using AdapterRemoval v2.2.1²² before transcript-level counts were obtained using kallisto v0.43.1.²³ Gene annotations for Rnor_6.0 were obtained from Ensembl Release 96 (European Bioinformatics Institute, UK). Transcript-level counts were summarized to the gene level, then analyzed using voom-precision weights method, incorporating additional sample-level weights.²⁴ Differentially expressed (DE) genes were considered to be

those with a false discovery rate (FDR)-adjusted p -value < 0.05 .

FDR thresholds of 5% and 10.0% were used to identify genes as potentially DE. Gene set enrichment analysis (GSEA) was also performed²⁵ as implemented in the fgsea package,²⁶ which has no requirement for formal consideration of genes as DE. For this, genes were ranked by their respective t -statistic and genes from hallmark gene sets were tested for enrichment at either end of the ranked list.²⁷ A Bonferroni-adjusted p -value < 0.05 was used to consider a gene set as enriched within the ranked list of genes. All analytic code is available at https://github.com/UofABioinformaticsHub/20180328_Atkins_RatFracture.

Statistical analysis. Statistical analyses of differences between the ZDF and WT rats were generated using voom-precision weights and moderated t -statistics as implemented in the limma package.²⁸ An FDR-adjusted p -value of < 0.05 was considered to be statistically significant.

Results

Delayed healing in fractured ZDF rats. At three weeks post-femoral osteotomy, radiological analysis of the callus formation of the fractured femur demonstrated delayed healing in the diabetic cohort (Figure 1). Callus formation was delayed in all six of the diabetic cohort compared to the six non-diabetic controls. The quality of the callus formed within the diabetic group clearly shows inconsistent fracture healing via increased areas

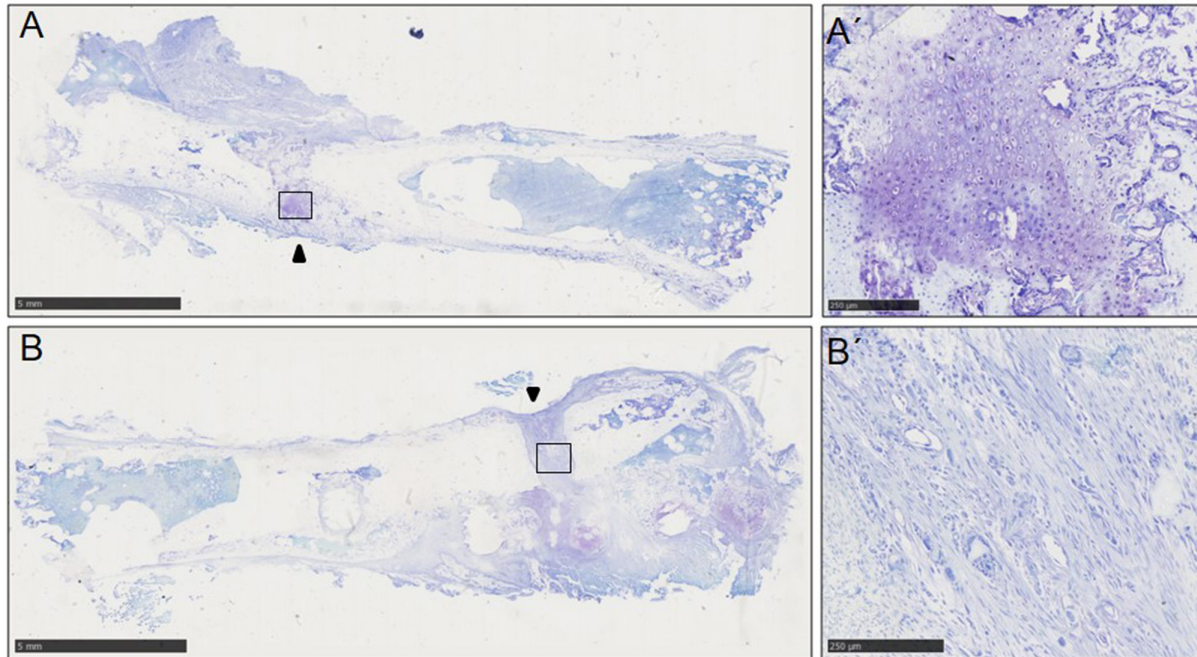


Fig. 2

Toluidine blue histology of whole femora of control (A) and Zucker diabetic fatty (B) rats three weeks post-fracture fixation. A' and B' show respective magnified regions indicated by black rectangles. Osteotomy sites are indicated by black triangles. The black arrow indicates the location of the fracture site. The black bars in A and B represent a length of 5 mm, while in A' and B' they represent 250 μ m.

of translucency within the callus formed. Delayed union is clearly evident, as suggested by irregular joint fracture space compared to the control rats. External fixators of the fractured femora are in situ, as demonstrated by the radio-opacity (Figure 1).

Histological analysis of fracture repair. WT control fracture sites showed clear evidence of near complete healing, with endochondral ossification tissue traversing the intramedullary space (Figures 2A and 2A'). ZDF fractures showed incomplete or little repair, with large fibrotic ingrowths to the fracture site (Figures 2B and 2B').

Gene expression analysis. Using differential mRNA-Seq analyses, 13,160 genes were considered as detected from the fracture site (Figure 3). Using a FDR of 0.05, only seven genes were found to be DE in ZDF callus, including *Patatin-like phospholipase domain containing protein 2* (*Pnpla2*), downregulated 7.39-fold (FDR = 0.006), and *LOC100909761*, now identified as *Myot*, the gene encoding the myocyte axon guidance product myotilin, which was upregulated 6.26-fold (FDR = 0.006).

Using a less stringent FDR threshold of 10.0% gave weak-to-moderate support for a further six genes as potentially DE (Table I). This includes proinflammatory genes such as the *Cxcl* group (*Cxcl1*, *Cxcl2*, *Cxcl3*), *Ccl20*, *interleukin (IL)-6*, and *TNFSF8*, which were significantly elevated. Only two genes were downregulated in this analysis, *Rcor2* and *Pnpla2* (Table I).

To gain further insight into the GE pathways differentially regulated in this model, GSEA was also performed (Table II). Of the 13 hallmark pathways identified as

enriched, nine were enriched for upregulated genes, including interferon-gamma response, tumour necrosis factor alpha (TNF- α) signalling via nuclear factor kappa B (NF- κ B), inflammatory response, and IL-6 JAK/STAT3 signalling, and all were associated with increased inflammation in the ZDF fracture callus. Three other pathways enriched for upregulated genes were epithelial-mesenchymal transition, myogenesis, and hypoxia, potentially indicating a disrupted cell differentiation or tissue repair response. Of the four pathways enriched for downregulated genes, G2M checkpoint, Myc targets V1, and E2f targets suggest impaired cell cycle progression. Overall, the GE analysis suggests a proinflammatory response associated with impaired or inappropriate tissue regeneration in the ZDF fractures.

Discussion

In this study, ZDF rats showed delayed or deficient fracture healing upon radiological and histological analysis of the callus. Radiological analyses (Figure 1) demonstrated disorganized mineralization and lack of union in ZDF fracture sites compared to WT littermates three weeks post-femoral osteotomy, indicated by unequal callus thickness and a polymorphic appearance. Histological analysis showed extensive fibrotic ingrowth within the callus of ZDF rats, compared to evidence of the expected endochondral fracture repair process in WT rats.

We sought to identify localized molecular mechanisms underlying aberrant fracture healing in this

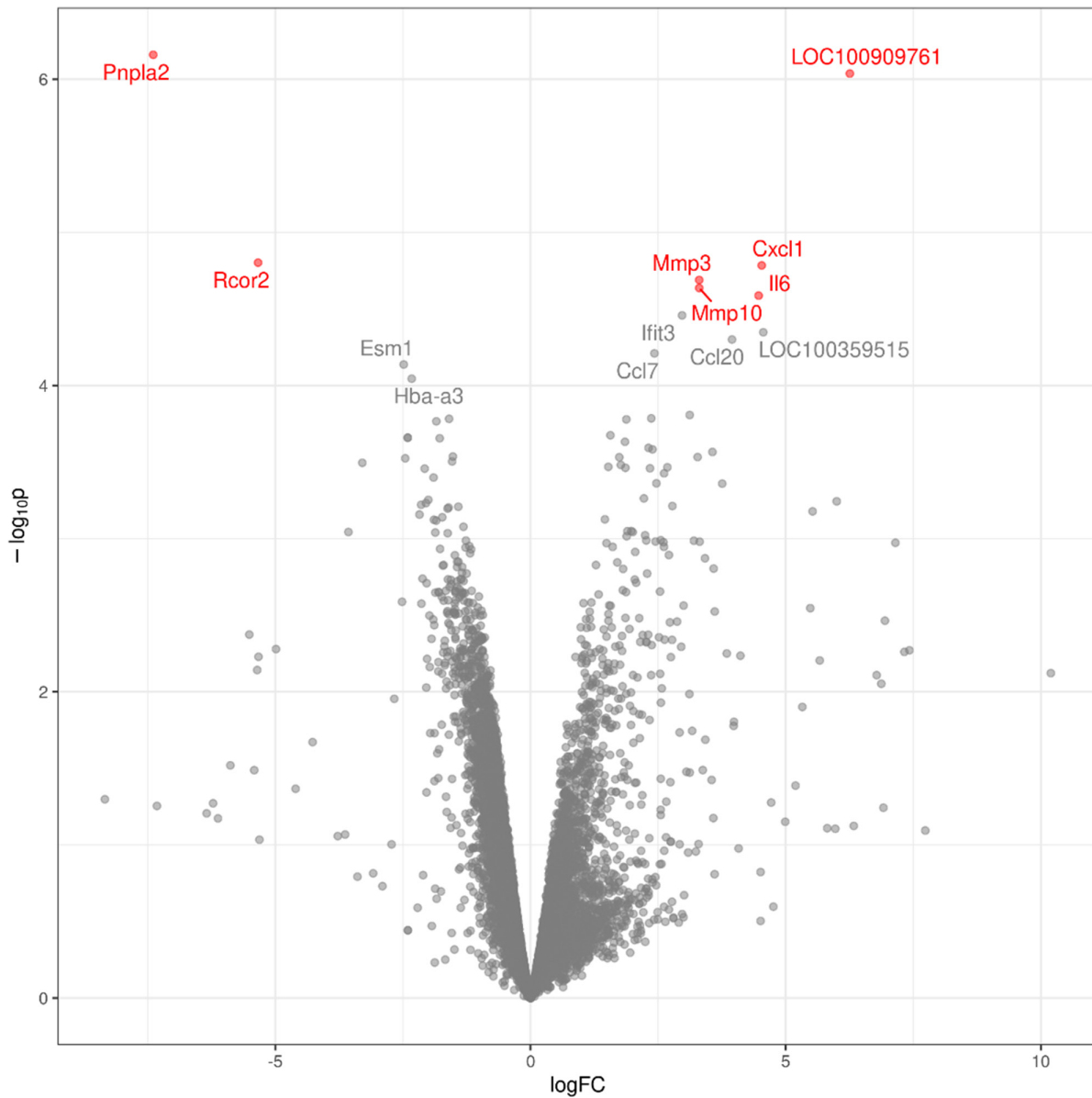


Fig. 3

Volcano plot with significant genes shown in red ($FDR < 0.05$). Genes to a FDR of 10.0% are additionally labelled in grey. FDR , false discovery rate; Mmp , matrix metalloproteinase; $Pnpla2$, Patatin-like phospholipase domain-containing protein 2.

diabetic model. mRNA-Seq analysis revealed seven DE genes ($FDR < 0.05$), with the two most highly-ranked being *Pnpla2* and *LOC100909761/Myot*. *Pnpla2* is a gene that encodes patatin-like phospholipase domain-containing protein 2, also known as adipose triglyceride lipase (ATGL), an enzyme responsible for intracellular hydrolysis of stored triglycerides.²⁹ *Pnpla2* was associated with non-alcoholic fatty liver disease in an obese population and developing renal complications within a diabetic population.^{30,31} Kim et al³² demonstrated that ATGL/*Pnpla2* expression is downregulated by insulin and TNF- α in adipocytes at both protein and mRNA levels. This correlates with the findings of our study, with the downregulation of

Pnpla2 mRNA likely reflecting the hyperinsulinaemic and hyperinflammatory state of diabetic rodents. *LOC100909761/Myot* was strongly upregulated in the ZDF callus. The significance of this is unclear but could reflect inappropriate mesenchymal differentiation away from osteogenic lineages (chondroblast-osteoblast) towards myoblast, as the gene product myotilin is best characterized as a protein involved in striated muscle contraction.³³ Further evidence for aberrant cell differentiation was obtained when GSEA of the entire gene set was performed (Table II). Of the top 13 hallmark gene pathway sets identified, epithelial-mesenchymal transition and myogenesis were positively associated with the tissue response in ZDF callus.

Table 1. The top 13 differentially expressed genes in whole femur rat messenger RNA sequencing of Zucker diabetic fatty compared to wild-type three weeks post-fracture fixation.

Gene name	Gene symbol	Expression in ZDF	logFC	p-value	FDR
Patatin-like phospholipase domain-containing protein 2	<i>Pnpla2</i>	down	7.39	6.92E-07	0.006
LOC100909761/myotilin	<i>Myot</i>	up	6.26	9.18E-07	0.006
REST corepressor 2	<i>Rcor2</i>	down	5.34	1.58E-05	0.049
C-X-C motif chemokine ligand 1	<i>Cxcl1</i>	up	4.53	1.64E-05	0.049
Matrix metalloproteinase 3	<i>Mmp3</i>	up	3.30	2.05E-05	0.049
Matrix metalloproteinase 10	<i>Mmp10</i>	up	3.31	2.31E-05	0.049
Interleukin-6	<i>Il-6</i>	up	4.47	2.59E-05	0.049
Interferon-induced protein with tetratricopeptide repeats 3	<i>Lfit3</i>	up	2.97	3.48E-05	0.057
LOC100359515/nitric oxide synthase 2, pseudogene 1	<i>Nos2-ps1</i>	up	4.56	4.49E-05	0.066
C-C motif chemokine ligand 20	<i>Ccl20</i>	up	3.95	5.01E-05	0.066
C-C motif chemokine ligand 7	<i>Ccl7</i>	up	2.43	6.17E-05	0.074
Endothelial cell specific molecule 1	<i>Esm1</i>	down	2.48	7.29E-05	0.080
Hemoglobin alpha, adult chain 3	<i>Hba-a3</i>	down	2.33	9.02E-05	0.091

FDR, false discovery rate; logFC, log fold-change; ZDF, Zucker diabetic fatty.

When applying a less stringent FDR of 0.1, six additional DE genes were identified (Table 1). A striking feature from this analysis was evidence of an inappropriate inflammatory response in the ZDF callus. Inflammation is an expected feature of fracture and of the healing response; under normal physiological conditions, inflammatory signals result in a local increase in macrophages, which release proinflammatory mediators such as IL-6 and CXCL chemokines that promote fracture healing.^{34,35} Proinflammatory cytokines are known to show peak expression within the first 24 hours after fracture, depressed levels during cartilage formation, and their levels increase again during bone remodelling.³⁶ Indeed, activating this initial inflammatory pathway is pivotal in fracture healing. The deficiency of inflammation caused by therapeutic agents such as non-steroidal anti-inflammatory drugs (NSAIDs) and corticosteroids is known to delay fracture healing time and increase the risk of nonunion.^{37–39} IL-6 is pivotal in the local immune response after fracture by regulating the recruitment of immune cells to the fracture haematoma, and by inducing regenerative processes augmenting bone repair.⁴⁰ IL-6 also regulates the differentiation of both osteoblasts and osteoclasts, and promotes angiogenesis by stimulating the release of vascular endothelial growth factor (VEGF).⁴¹ The importance of this cytokine in fracture healing was exemplified by studies in IL-6 knockout mice, which demonstrated delayed fracture healing with decreased osteoclastogenesis and impaired callus formation.^{42,43} Therefore, it is indisputable that inflammation is crucial in the bone healing process and that suppression of inflammatory cytokine expression forms an unfavourable microenvironment in the fracture site to prolong healing.

In contrast, a prolonged proinflammatory phase, as evident in the fracture healing cascade in ZDF rats at three weeks post-fracture in this study, is associated with impaired bone repair. Acute inflammation due to severe

injuries such as polytrauma and open fracture can lead to pronounced TNF- α and IL-6 expression, and has a detrimental effect on bone healing.^{44–46} GSEA in our study indicated that within the diabetic rat cohort, upregulation of the inflammatory gene sets interferon-gamma response, TNF- α signalling via NF- κ B, inflammatory response, and IL-6 JAK/STAT3 occurred or persisted even after three weeks. Furthermore, the analysis showed significantly upregulated individual GE of *Il6* and *Mmp3* with a log fold-change value of 4.47 and 3.30, respectively. As aforementioned, while IL-6 has an important role in fracture healing, over-production can inhibit canonical Wnt/ β -catenin activity, an essential pathway for osteoblast differentiation.⁴⁷ Wu et al⁴⁸ also suggested that IL-6 enhances osteoclastogenesis by excessive promotion of JAK2 and RANKL activity. Moreover, IL-6 has been shown to stimulate osteoclastogenesis and bone resorption directly,⁴⁹ with IL-6-overexpressing mice found to have osteopenia and defective ossification.⁵⁰

An increased inflammatory state within the ZDF fracture callus is further supported by the increased GE of *Angptl4* and *Lfit3*, which are involved in inflammation in patients with T2DM and interferon-gamma signalling.^{51,52} Alvarez-López et al⁵³ described the association between *Rcor2* downregulation and increased inflammation, consistent with our findings. GE of the CXC chemokine group, including *Cxcl1* (FDR = 0.049), *Cxcl2* (FDR = 0.188), and *Cxcl3* (FDR = 0.164), was also upregulated in the diabetic rat cohort (Table 1). These chemokines are collectively known as potent neutrophil chemoattractants and are involved in cancer metastasis, angiogenesis, and wound healing.^{54–56} CXCL1 forms complex interactions with glycosaminoglycans (GAG) on endothelial cells and the extracellular matrix (ECM), resulting in chemotactic gradients that modulate neutrophil recruitment to the site of inflammation.⁵⁷ Although neutrophils have a crucial role in the systemic immune response, and despite being the most abundant immune cell type in the early

Table II. Top 13 enriched Hallmark gene sets using a Bonferroni-adjusted p-value < 0.01. The normalized enrichment score indicates which end of the ranked list appeared to be enriched for each gene set, with negative values indicating the downregulated genes. The number of genes in the gene set is also indicated, as is the number of genes at the point of maximum enrichment. The most highly ranked genes before the point of maximal enrichment are given in the final column.

Hallmark pathway	p-value	Adjusted p-value	NES	Size, n	Size at max, n	Genes
Epithelial-mesenchymal transition	8.83E-28	1.72E-23	3.27	173	89	<i>Cxcl1; Mmp3; Il6; Cxcl3; Cxcl2; Cxcl6; Acta2; Fbln2; Tgfb; Htra1; Timp1; Mgp; Ptx3; Tagln; Mfap5; Col5a3; Inhba; Tfp2</i>
TNF- α signalling via NF- κ B	1.73E-27	3.35E-23	3.25	173	83	<i>Cxcl1; Il6; Ccl20; Cxcl3; Il1b; Cxcl2; Cxcl6; Tlr2; Ptgs2; Tnfaip6; G0s2; F3; Sod2; Olr1; Il1a; Pde4b; Ptx3; Gfpt2</i>
Inflammatory response	7.75E-23	1.51E-18	3.10	156	59	<i>Il6; Ccl20; Ccl7; Il1b; Cxcl6; Tlr2; Has2; Tnfaip6; F3; Olr1; Slc7a2; Il1r1; Il1a; Pde4b; Timp1; Ifitm3; Inhba; Hif1a</i>
E2f targets	6.24E-20	1.21E-15	2.40	193	129	<i>Birc5; Ran; Srsf2; Kif18b; Cdc25b; Rrm2; Rad51ap1; Cdc3; Pold2; Ncapd2; Stmn1; Ppm1d; Dclre1b; Ccne1; E2f8; Prps1; H2afx; Gins3</i>
Heme metabolism	3.51E-19	6.82E-15	2.40	175	98	<i>Bpgm; Minpp1; Mkrn1; Klfl1; Foxo3; Abcb6; Cdr2; Fbxo7; Fech; Alas2; Ctse; Epb41; Gclm; Epb42; Ranbp10; Prdx2; Cpox; Hagh</i>
Myogenesis	2.93E-16	5.69E-12	2.67	165	61	<i>Mylp; Myl1; Myoz1; Tnni2; Myh1; Myom2; Eno3; Ckm; Pgam2; Tnnt3; Tagln; Tnnc2; Cox6a2; Pvalb; Mb; Col3a1; Actn3; Hspb8</i>
Coagulation	3.11E-13	6.04E-09	2.78	93	33	<i>Mmp3; Mmp10; Ctsl; Cfi; C1s; F3; Plat; Olr1; Htra1; Timp1; LOC100911545; Tfp2; Maff; C1qa; Mmp2; Ctsk; Serpine1; C2</i>
IL-6 JAK/STAT3 signalling	1.09E-12	2.12E-08	2.85	75	20	<i>Cxcl1; Il6; Ccl7; Cxcl3; Il1b; Cxcl2; Tlr2; Il1r2; Cxcl13; Il1r1; LOC100911545; Osmr; Cd14; Tnfrsf12a; Il2ra; Il4r; Csf3r; Pf4</i>
G2M checkpoint	3.08E-12	5.98E-08	2.11	189	107	<i>Hira; Birc5; Srsf2; Ccna2; Tent4a; Cdc25b; Stmn1; Tgfb1; H2afx; Aurka; E2f3; Racgap1; E2f4; Hnrnpd; Mcm5; Ccnf; Cul4a; Cdkn2c</i>
Complement	7.26E-11	1.41E-06	2.30	158	37	<i>Cxcl1; Il6; Cxcl3; Ctsl; Cxcl2; C1s; F3; Plat; Olr1; Ctss; Timp1; Ctsc; Tfp2; Maff; C1qa; Col4a2; Pla2g7; Zfpm2</i>
Hypoxia	5.24E-09	1.02E-04	2.14	171	49	<i>Il6; Angptl4; F3; Errf1; Eno3; Slc2a1; Tgfb; Pgam2; Plin2; Ddit4; Ier3; Atf3; Maff; Pygm; Prdx5; Cdkn1a; Fos; Tgm2</i>
Myc targets V1	1.08E-08	2.10E-04	1.90	194	101	<i>Ran; Srsf2; Pabpc4; Ccna2; Tufm; Pold2; Pabpc1; Ppm1g; Phb2; Cstf2; Snrpa1; Hnrnpd; Mcm5; Mcm7; Trim28; Impdh2; Prdx3; Rpl14</i>
Interferon-gamma response	3.29E-08	6.40E-04	2.03	173	39	<i>Il6; Ifit3; Ccl7; Ptgs2; C1s; Tnfaip6; Sod2; Pde4b; Ifitm3; Upp1; Mx1; Hif1a; Cdkn1a; Cd274; Il4r; Ifit2; C2; Icam1</i>

IL, interleukin; NES, normalized enrichment score; NF- κ B, nuclear factor kappa B; Size, number of genes in the gene set; Size at max, number of genes at the point of maximum enrichment; TNF, tumour necrosis factor alpha.

fracture haematoma, excessive or prolonged influx of neutrophils into the fracture haematoma can have a negative impact on fracture healing after systemic inflammation.⁵⁸ Furthermore, rats with a 60% decrease

in neutrophils from the administration of neutrophil-neutralizing antiserum showed enhanced osteoblastic differentiation, supporting the conclusion that the neutrophil-mediated inflammatory response appears

to suppress osteoblastic differentiation.⁵⁹ In the ZDF fractured femora, there was clear evidence of a pannus-like fibrotic ingrowth at the fracture site, containing polymorphs likely to be neutrophils. Together, the data from our study suggest that delayed bone healing in ZDF fractures is likely to be caused by elevated inflammatory mediator expression.

This study has some limitations. We only compared GE profiles between fractured ZDF and WT bone, and did not adjust for pre-existing differences in GE between these genotypes. Furthermore, we only examined GE at a single timepoint, albeit at the highly informative timepoint of three weeks postoperative, providing a snapshot rather than a progression of GE profiles throughout the healing phase. In this sense, we consider our study to be a pilot, giving proof of the concept of the model. The samples examined by mRNA-Seq contained various cell types, which varied between genotypes thus limiting the statistical power of the study; in future studies, it may be possible to use techniques such as laser capture microdissection to analyze cell type-specific GE changes. We also could not determine the cause or effect of GE changes from this analysis. Furthermore, we only examined mRNA changes and did not consider alterations in non-coding RNA types or resulting protein expression levels. However, to our knowledge, this is the first study of GE in the ZDF model during the fracture healing phase. By using unbiased GSEA, we were able to show significantly upregulated inflammatory gene pathway expression within the fracture callus. As the GE profiles for the ZDF rats are highly consistent with those observed in human patients,⁶⁰ we believe that this study will aid in understanding the delayed fracture healing phenomenon seen in diabetic patients. Further study is required to confirm whether these same genes are similarly associated in humans, and whether the identified genes are causative of delayed healing, or a product of it.

The findings have implications for the management of fracture healing in diabetic patients. The aberrant healing process and molecular mechanisms identified could potentially serve as targets for future therapeutic interventions to enhance fracture repair in this patient population. Further research should investigate whether modulation of the identified pathways (Pnpla2 and LOC100909761/Myot) can improve outcomes. Additionally, the potential links highlighted in this study between diabetes, aberrant localized mesenchymal differentiation, and impaired fracture healing may stimulate further exploration into the broader effects of diabetes on tissue regeneration and repair.

In conclusion, ZDF rodent callus showed persistent upregulation of pro-inflammatory and pro-chemotactic GE, such as *IL-6*, *Cxcl1*, *Ccl7*, and *Ccl20*. Such increased inflammation can delay fracture healing by complex mechanisms involving excessive neutrophil migration and increased osteoclastogenesis, resulting in disorganized mineralization of the callus.

Supplementary material



An ARRIVE checklist is included to show that the ARRIVE guidelines were adhered to in this study.

References

- No authors listed.** Diabetes. World Health Organization. 2021. <https://www.who.int/news-room/fact-sheets/detail/diabetes> (date last accessed 22 September 2023).
- Carnevale V, Romagnoli E, D'Erasmo E.** Skeletal involvement in patients with diabetes mellitus. *Diabetes Metab Res Rev.* 2004;20(3):196–204.
- Loder RT.** The influence of diabetes mellitus on the healing of closed fractures. *Clin Orthop Relat Res.* 1988;232:210–216.
- Folk JW, Starr AJ, Early JS.** Early wound complications of operative treatment of calcaneus fractures: analysis of 190 fractures. *J Orthop Trauma.* 1999;13(5):369–372.
- Retzepi M, Donos N.** The effect of diabetes mellitus on osseous healing. *Clin Oral Implants Res.* 2010;21(7):673–681.
- Marin C, Luyten FP, Van der Schueren B, Kerckhofs G, Vandamme K.** The impact of type 2 diabetes on bone fracture healing. *Front Endocrinol (Lausanne).* 2018;9:6.
- Ding K-H, Wang Z-Z, Hamrick MW, et al.** Disordered osteoclast formation in RAGE-deficient mouse establishes an essential role for RAGE in diabetes related bone loss. *Biochem Biophys Res Commun.* 2006;340(4):1091–1097.
- Liu R, Bal HS, Desta T, et al.** Diabetes enhances periodontal bone loss through enhanced resorption and diminished bone formation. *J Dent Res.* 2006;85(6):510–514.
- Pacios S, Kang J, Galicia J, et al.** Diabetes aggravates periodontitis by limiting repair through enhanced inflammation. *FASEB J.* 2012;26(4):1423–1430.
- Davoren P.** Glucose-lowering medicines for type 2 diabetes. *Aust Fam Physician.* 2015;44(5):176–179.
- Das UN, Rao AA.** Gene expression profile in obesity and type 2 diabetes mellitus. *Lipids Health Dis.* 2007;6:35.
- Sreekumar R, Halvatsiotis P, Schimke JC, Nair KS.** Gene expression profile in skeletal muscle of type 2 diabetes and the effect of insulin treatment. *Diabetes.* 2002;51(6):1913–1920.
- Owens DR.** Spontaneous, Surgically and Chemically Induced Models of Disease. In: Suckow MA, Weisbroth SH, Franklin CL, eds. *The Laboratory Rat: American College of Laboratory Animal Medicine Series.* Second ed. Cambridge, Massachusetts: Elsevier, 2006: 711–732. . Second ed.
- Yorek MA.** Alternatives to the streptozotocin-diabetic rodent. *Int Rev Neurobiol.* 2016;127:89–112.
- Liu C, Liu Y, Yu Y, Zhao Y, Zhang D, Yu A.** Identification of up-regulated ANXA3 resulting in fracture non-union in patients with T2DM. *Front Endocrinol (Lausanne).* 2022;13:890941.
- Takahara S, Lee SY, Iwakura T, et al.** Altered expression of microRNA during fracture healing in diabetic rats. *Bone Joint Res.* 2018;7(2):139–147.
- Harrison LJ, Cunningham JL, Strömberg L, Goodship AE.** Controlled induction of a pseudarthrosis: a study using a rodent model. *J Orthop Trauma.* 2003;17(1):11–21.
- Anderson PH, Sawyer RK, Moore AJ, May BK, O'Loughlin PD, Morris HA.** Vitamin D depletion induces RANKL-mediated osteoclastogenesis and bone loss in a rodent model. *J Bone Miner Res.* 2008;23(11):1789–1797.
- Ormsby RT, Zelmer AR, Yang D, et al.** Evidence for osteocyte-mediated bone-matrix degradation associated with periprosthetic joint infection (PJI). *Eur Cell Mater.* 2021;42:264–280.
- Anderson PH, Iida S, Tyson JHT, Turner AG, Morris HA.** Bone CYP27B1 gene expression is increased with high dietary calcium and in mineralising osteoblasts. *J Steroid Biochem Mol Biol.* 2010;121(1–2):71–75.
- Ward CM, To T-H, Pederson SM.** ngsReports: a Bioconductor package for managing FastQC reports and other NGS related log files. *Bioinformatics.* 2020;36(8):2587–2588.
- Schubert M, Lindgreen S, Orlando L.** AdapterRemoval v2: rapid adapter trimming, identification, and read merging. *BMC Res Notes.* 2016;9:88.
- Bray NL, Pimentel H, Melsted P, Pachter L.** Erratum: Near-optimal probabilistic RNA-seq quantification. *Nat Biotechnol.* 2016;34(8):888.
- Law CW, Chen Y, Shi W, Smyth GK.** voom: Precision weights unlock linear model analysis tools for RNA-seq read counts. *Genome Biol.* 2014;15(2):R29.
- Subramanian A, Tamayo P, Mootha VK, et al.** Gene set enrichment analysis: a knowledge-based approach for interpreting genome-wide expression profiles. *Proc Natl Acad Sci U S A.* 2005;102(43):15545–15550.
- Korotkevich G, Sukhov V, Budin N, Shpak B, Artyomov MN, Sergushichev A.** Fast gene set enrichment analysis. *bioRxiv.* 2021.

27. Liberzon A, Birger C, Thorvaldsdóttir H, Ghandi M, Mesirov JP, Tamayo P. The Molecular Signatures Database (MSigDB) hallmark gene set collection. *Cell Syst*. 2015;1(6):417–425.
28. Ritchie ME, Phipson B, Wu D, et al. limma powers differential expression analyses for RNA-sequencing and microarray studies. *Nucleic Acids Res*. 2015;43(7):e47.
29. Schreiber R, Xie H, Schweiger M. Of mice and men: The physiological role of adipose triglyceride lipase (ATGL). *Biochim Biophys Acta Mol Cell Biol Lipids*. 2019;1864(6):880–899.
30. Zegers D, Verrijken A, Beckers S, et al. Association study of PNPLA2 gene with histological parameters of NAFLD in an obese population. *Clin Res Hepatol Gastroenterol*. 2016;40(3):333–339.
31. Zhao H, Zhang H, Wang Y, et al. Association between PNPLA2 gene polymorphisms and the risk of diabetic kidney disease in a Chinese Han population with type 2 diabetes. *J Diabetes Res*. 2020;2020:5424701.
32. Kim JY, Tillison K, Lee JH, Rearick DA, Smas CM. The adipose tissue triglyceride lipase ATGL/PNPLA2 is downregulated by insulin and TNF-alpha in 3T3-L1 adipocytes and is a target for transactivation by PPARgamma. *Am J Physiol Endocrinol Metab*. 2006;291(1):E115–27.
33. Kostan J, Pavšič M, Puž V, et al. Molecular basis of F-actin regulation and sarcomere assembly via myotilin. *PLoS Biol*. 2021;19(4):e3001148.
34. Mountziaris PM, Mikos AG. Modulation of the inflammatory response for enhanced bone tissue regeneration. *Tissue Eng Part B Rev*. 2008;14(2):179–186.
35. Baht GS, Vi L, Alman BA. The role of the immune cells in fracture healing. *Curr Osteoporos Rep*. 2018;16(2):138–145.
36. Dimitriou R, Tsiridis E, Giannoudis PV. Current concepts of molecular aspects of bone healing. *Injury*. 2005;36(12):1392–1404.
37. Su B, O'Connor JP. NSAID therapy effects on healing of bone, tendon, and the enthesis. *J Appl Physiol (1985)*. 2013;115(6):892–899.
38. Wheatley BM, Nappo KE, Christensen DL, Holman AM, Brooks DI, Potter BK. Effect of NSAIDs on bone healing rates: A meta-analysis. *J Am Acad Orthop Surg*. 2019;27(7):e330–e336.
39. Liu Y-Z, Akhter MP, Gao X, et al. Glucocorticoid-induced delayed fracture healing and impaired bone biomechanical properties in mice. *Clin Interv Aging*. 2018;13:1465–1474.
40. Kaiser K, Prystaz K, Vikman A, et al. Pharmacological inhibition of IL-6 trans-signaling improves compromised fracture healing after severe trauma. *Naunyn Schmiedebergs Arch Pharmacol*. 2018;391(5):523–536.
41. Cohen T, Nahari D, Cerem LW, Neufeld G, Levi BZ. Interleukin 6 induces the expression of vascular endothelial growth factor. *J Biol Chem*. 1996;271(2):736–741.
42. Yang X, Ricciardi BF, Hernandez-Soria A, Shi Y, Pleshko Camacho N, Bostrom MPG. Callus mineralization and maturation are delayed during fracture healing in interleukin-6 knockout mice. *Bone*. 2007;41(6):928–936.
43. Wallace A, Cooney TE, Englund R, Lubahn JD. Effects of interleukin-6 ablation on fracture healing in mice. *J Orthop Res*. 2011;29(9):1437–1442.
44. Reinke S, Geissler S, Taylor WR, et al. Terminally differentiated CD8⁺ T cells negatively affect bone regeneration in humans. *Sci Transl Med*. 2013;5(177):177ra36.
45. Valparaiso AP, Vicente DA, Bograd BA, Elster EA, Davis TA. Modeling acute traumatic injury. *J Surg Res*. 2015;194(1):220–232.
46. Andrzejowski P, Giannoudis PV. The “diamond concept” for long bone non-union management. *J Orthop Traumatol*. 2019;20(1):21.
47. Li X, Zhou Z-Y, Zhang Y-Y, Yang H-L. IL-6 contributes to the defective osteogenesis of bone marrow stromal cells from the vertebral body of the glucocorticoid-induced osteoporotic mouse. *PLoS One*. 2016;11(4):e0154677.
48. Wu Q, Zhou X, Huang D, Ji Y, Kang F. IL-6 enhances osteocyte-mediated osteoclastogenesis by promoting JAK2 and RANKL activity in vitro. *Cell Physiol Biochem*. 2017;41(4):1360–1369.
49. Kwan Tat S, Padrines M, Théoleyre S, Heymann D, Fortin Y. IL-6, RANKL, TNF-alpha/IL-1: interrelations in bone resorption pathophysiology. *Cytokine Growth Factor Rev*. 2004;15(1):49–60.
50. De Benedetti F, Rucci N, Del Fattore A, et al. Impaired skeletal development in interleukin-6-transgenic mice: a model for the impact of chronic inflammation on the growing skeletal system. *Arthritis Rheum*. 2006;54(11):3551–3563.
51. Tjeerdema N, Georgiadi A, Jonker JT, et al. Inflammation increases plasma angiopoietin-like protein 4 in patients with the metabolic syndrome and type 2 diabetes. *BMJ Open Diabetes Res Care*. 2014;2(1):e000034.
52. No authors listed. IFIT3 Gene - Interferon Induced Protein With Tetratricopeptide Repeats 3. GeneCards. 2023. <https://www.genecards.org/cgi-bin/carddisp.pl?gene=IFIT3> (date last accessed 22 September 2023).
53. Alvarez-López MJ, Molina-Martínez P, Castro-Freire M, et al. Rcor2 underexpression in senescent mice: a target for inflammaging? *J Neuroinflammation*. 2014;11:126.
54. Romagnani P, Lasagni L, Annunziato F, Serio M, Romagnani S. CXC chemokines: the regulatory link between inflammation and angiogenesis. *Trends Immunol*. 2004;25(4):201–209.
55. Doll D, Keller L, Maak M, et al. Differential expression of the chemokines GRO-2, GRO-3, and interleukin-8 in colon cancer and their impact on metastatic disease and survival. *Int J Colorectal Dis*. 2010;25(5):573–581.
56. Zaja-Milatovic S, Richmond A. CXC chemokines and their receptors: a case for a significant biological role in cutaneous wound healing. *Histol Histopathol*. 2008;23(11):1399–1407.
57. Sawant KV, Poluri KM, Dutta AK, et al. Chemokine CXCL1 mediated neutrophil recruitment: Role of glycosaminoglycan interactions. *Sci Rep*. 2016;6:33123.
58. Kovtun A, Bergdolt S, Wiegner R, Radermacher P, Huber-Lang M, Ignatius A. The crucial role of neutrophil granulocytes in bone fracture healing. *Eur Cell Mater*. 2016;32:152–162.
59. Chung R, Cool JC, Scherer MA, Foster BK, Xian CJ. Roles of neutrophil-mediated inflammatory response in the bony repair of injured growth plate cartilage in young rats. *J Leukoc Biol*. 2006;80(6):1272–1280.
60. Patel D, Rooney R, Groom S. Gene Expression Profiles for the Zucker Fatty Rat Versus Zucker Diabetic Fatty Rat are Highly Consistent with Those Observed in Human Patients. Charles River Laboratories. 2006. <https://www.criv.com/sites/default/files/resources/GeneExpressionProfilesfortheZuckerFattyRatVersusZuckerDiabeticFattyRatAreHighlyConsistentwithThoseObservedinHumanPatients.pdf> (date last accessed 22 September 2023).

Author information:

- J. Sung, MBBS (Bachelor of Medicine, Bachelor of Surgery), Clinical Associate Lecturer
- G. J. Atkins, PhD, FIOR, Professor of Orthopaedic Research
- P. J. Smitham, PhD, FRCS (Tr & Orth), FRACS, Consultant Orthopaedic Surgeon, Associate Professor
Centre for Orthopaedic and Trauma Research, Adelaide Medical School, Faculty of Health and Medical Sciences, The University of Adelaide, Adelaide, Australia.
- K. R. Barratt, BPha (Bachelor of Pharmacy), Research Scientist
- P. H. Anderson, BSc (Bachelor of Science), Associate Research Professor, Professorial Lead, Clinical and Health Sciences
Clinical and Health Sciences, University of South Australia, Adelaide, Australia.
- S. M. Pederson, PhD, BMA & CompSc (Hons) (Bachelor of Maths and Computer Science), BSc (Bachelor of Science), BMus (Bachelor of Music), Bioinformatician, Co-ordinator - Bioinformatics Hub, Bioinformatics Hub, School of Biological Sciences, The University of Adelaide, Adelaide, Australia; Black Ochre Data Labs, Indigenous Genomics, Telethon Kids Institute, Adelaide, Australia.
- C. Chenu, PhD, Professor of Skeletal Biology
- I. Reichert, FRCS (Tr & Orth), MD, PhD, Consultant Trauma & Orthopaedic Surgeon
The Royal Veterinary College, London, UK.

Author contributions:

- J. Sung: Data curation, Methodology, Writing – original draft, Writing – review & editing.
- K. R. Barratt: Data curation, Methodology, Investigation.
- S. M. Pederson: Conceptualization, Formal analysis, Investigation, Methodology, Software, Validation, Writing – review & editing.
- C. Chenu: Investigation, Methodology, Resources, Supervision, Validation.
- I. Reichert: Formal analysis, Investigation, Methodology.
- G. J. Atkins: Conceptualization, Data curation, Formal analysis, Investigation, Methodology, Resources, Supervision, Validation, Writing – review & editing.
- P. H. Anderson: Conceptualization, Data curation, Formal analysis, Investigation, Methodology, Resources, Supervision, Writing – review & editing.
- P. J. Smitham: Conceptualization, Formal Analysis, Funding acquisition, Investigation, Methodology, Project administration, Supervision, Validation, Writing - review & editing.

Funding statement:

- The authors disclose receipt of the following financial or material support for the research, authorship, and/or publication of this article: this study was partly funded by a Joint Action grant from the British Orthopaedic Association (grant number: GA1273).

ICMJE COI statement:

- The authors report that this study was partly funded by a Joint Action grant from the British Orthopaedic Association (grant number: GA1273).

Data sharing:

- The datasets generated and analyzed in the current study are not publicly available due to data protection regulations. Access to data is limited to the researchers who have obtained permission for data processing. Further inquiries can be made to the corresponding author.

Ethical review statement:

- This study was approved by the University of South Australia Animal Ethics Committee (Approval No. U15-16).

Open access funding:

- The authors report that they received open access funding for their manuscript from the University of Adelaide.

© 2023 Author(s) et al. This is an open-access article distributed under the terms of the Creative Commons Attribution Non-Commercial No Derivatives (CC BY-NC-ND 4.0) licence, which permits the copying and redistribution of the work only, and provided the original author and source are credited. See <https://creativecommons.org/licenses/by-nc-nd/4.0/>